Available online at www.sciencedirect.com
ScienceDirect
Journal of Molecular Catalysis A: Chemical 260 (2006) 247–254
JOURNAL OF MOLECULAR CATALYSIS A: CHEMICAL
www.elsevier.com/locate/molcata

Synthesis of nanosized TiO_2 particles in reverse micelle systems and their photocatalytic activity for degradation of toluene in gas phase

Ryoji Inaba, Takayuki Fukahori, Masato Hamamoto, Teruhisa Ohno *

Department of Applied Chemistry, Faculty of Engineering, Kyushu Institute of Technology, 1-1 Sensuicho, Tobata, Kitakyushu 804-8550, Japan

Received 1 May 2006; received in revised form 27 June 2006; accepted 28 June 2006
Available online 17 August 2006

Abstract

Nanosized pure TiO_2 particles with high crystallinity and large surface area were prepared by hydrolysis of tetrabutyl titanate in water/Triton X-100/isooctane reverse micelle solutions as reaction media followed by hydrothermal treatment to improve crystallinity. The prepared TiO_2 nanoparticles were characterized by XRD, BET, TGA, FT-IR and TEM. The size of ultrafine particles was controlled by changing the water content of the reverse micelle solution. The TiO_2 particles showed monodispersity, large surface area and high degrees of crystallinity and thermostability. The photocatalytic activity of the TiO_2 particles was evaluated by decomposition of toluene in the gas phase. The activity of the TiO_2 nanoparticles was higher than that of commercially available anatase fine particles, such as ST-01, which is one of the most active photocatalysts for degradation of organic compounds in the gas phase.

Keywords: TiO_2; Photocatalyst; Reverse micelle method; Hydrothermal treatment

1. Introduction

Since the discovery of photoelectrochemical splitting of water on titanium dioxide (TiO_2) electrodes by Fujishima and Honda in 1972 [1], titanium dioxide has been intensively investigated as a photocatalyst. Many studies have focused on the degradation of hazardous and toxic organic compounds [2–8].

Much interest has been shown in photochemical reactions on TiO_2 particles due to their potential application in the conversion of solar energy into chemical energy [9–13] and electric energy [14,15]. When TiO_2 powder is irradiated with a photon energy larger than the band-gap energy, electrons (e^-) and holes (h^+) are generated in the conduction band and the valence band, respectively. These electrons and holes are thought to have the respective abilities to reduce and oxidize chemical species adsorbed on the surfaces of TiO_2 particles [8].

TiO_2 has three kinds of crystal structures: anatase, rutile and brookite. Anatase and brookite phases are thermodynamically metastable and can be transformed exothermally and irreversibly to the rutile phase at higher temperatures. The transition temperatures reported in the literature range from 450 to 1200 °C. The transformation temperature depends on the nature and structure of the precursor and the preparation conditions [6,16]. Among the three kinds crystal structure of TiO_2, commercially available anatase TiO_2 fine particles are the most active for photocatalytic degradation of organic compounds in the gas phase such as acetaldehyde.

Nano-materials with an average grain size less than 100 nm have been attracting much attention because they exhibit unique and improved mechanical, electrical, optical, and chemical properties compared with conventional polycrystalline materials. For the purpose of the functionalization of the materials, their chemical and physical properties should be fully controlled.

Various synthesis methods including the CVD method [17], colloidal template [2], hydrolysis [18,19], sol–gel [20–22], microemulsion (or reverse micelle systems) [6,16,23,24] and hydrothermal synthesis [25,26], have been used to prepare TiO_2 nanoparticles. The sol–gel method [27] requires costly organic solvents. The direct hydrolysis of titanium salts and chemical vapor deposition procedure in which $TiCl_4$ vapor is oxidized at very high temperatures (∼500 °C) can be used to prepare nanosized TiO_2 particles [28–30]. Compared with these methods, the preparation of TiO_2 nanoparticles using hydrothermal synthesis method could be conducted at a relatively low reaction tempera-

* Corresponding author. Fax: +81 93 884 3318.
E-mail address: tohno@che.kyutech.ac.jp (T. Ohno).

1381-1169/$ – see front matter © 2006 Elsevier B.V. All rights reserved.
doi:10.1016/j.molcata.2006.06.053

ture (∼250 °C) to generate a highly crystalline product without the necessity of post-synthesis calcination.

Reverse micelle systems (or water-in-oil microemulsions) have been used as microreactors to synthesize ultrafine particles with a narrow distribution of particle size by controlling the growth process [6]. Nanosized TiO_2 particles have also been prepared by microemulsion-mediated processing [4–6,24,31,32]. Reverse micelles (or water-in-oil microemulsions) are nanometer-scale surfactant association colloids formed in a nonpolar organic solvent. Polar solvents such as water are easily soluble inside reverse micelle because the inside of the reverse micelle is quite hydrophilic. In addition, they are a thermodynamically stable, isotropic, transparent mixture of oil and water separated by a thin surfactant monolayer. Reverse micelle systems provide a micro-heterogeneous medium for the generation of nanoparticles. A dimeric micelle is generated in a short lifetime by collision, and a chemical reaction occurs by substance exchange during the collision. By repeating this collision, a further chemical reaction proceeds and nucleus generation occurs. Furthermore, the nucleus grows up to be a fine particle when the hydrolyzed species collide.

Nanoparticles of metals such as Cu, Pt and Pd have been prepared by dissolving metal salts in the water pools of a reverse micelle system followed by the addition of a reducing reagent [3,33]. The technique for preparing nanoparticles has been used to prepare a polymer membrane doped with CdS [34] or stable ultrafine photocatalyst particles in various solvents [7]. The formation of particles in such systems is controlled by the reactant distribution in the water pools and by the dynamics of inner water pool exchange. Surfactant-stabilized microcavities provide sites for a nano-scale reaction that limit nucleation, growth and agglomeration of particles. However, TiO_2 nanoparticles prepared by the reverse micelle method do not show photocatalytic activity because they are amorphous. In order to show photocatalytic activity, amorphous TiO_2 nanoparticles should be calcined at rather higher temperature. At the same time, the organic contaminant remaining in the prepared TiO_2 using reverse micelle methods is removed by calcination. However, heat treatment of TiO_2 nanoparticles at a high temperature results in sintering, agglomeration, and phase transition from anatase to rutile.

TiO_2 nanoparticles prepared by a reverse micelle method followed by hydrothermal treatment can be crystallized at rather low temperature as compared with those followed by the general calcination treatment, and sintering of TiO_2 nanoparticles does not occur during the treatment. There have been several studies on hydrothermal synthesis of ultrafine TiO_2 powder [25,26]. By changing hydrothermal reaction conditions, such as pH and additives, crystalline products with different compositions, structures, and morphologies have been generated [25,26].

In this work, we attempted to produce monodispersed TiO_2 nanoparticles of high purity using a reverse micelle (RM) system composed of water, Triton X-100 (TX-100) and isooctane and by hydrothermal treatment. We studied the effects of the water content and calcination temperature on the crystal phase and particle size of TiO_2 nanoparticles. We also estimated the photocatalytic activity of the prepared TiO_2 nanoparticles for decomposition of toluene in the gas phase.

2. Experimental

2.1. Materials

TiO_2 powder having an anatase phase was obtained from Ishihara Sangyo (ST-01). The relative surface area of ST-01 was 285.3 m^2/g. TX-100 (*tert*-octylphenoxypolyethoxyethanol), isooctane (2,2,4-trimethyl-pentane, 99.0%) and toluene (99.5%) were obtained from Wako Pure Chemical Industries. Tetrabutyl titanate (97%) was purchased from Aldrich Chemical Co. All reagents were used without further purification. Water was distilled and deionized before use. Other chemicals were obtained from commercial sources as guaranteed reagents and were used without further purification.

2.2. Preparation of titanium dioxide

For the preparation of TiO_2 nanoparticles in the RM system, TX-100 was used as the surfactant and isooctane was used as the continuous oil phase. Tetrabutyl titanate was used as a titanium dioxide source. Preparation of titanium dioxide was carried out as follows.

The RM solution was prepared by dispersing the aqueous phase into the TX-100 (0.64 g, 2.5×10^{-3} mol)/isooctane (50 ml) mixture with vigorous stirring. During this process, the water content of the solution, W_o (=[H_2O]/[TX-100]), was controlled. In order to allow tetrabutyl titanate to react with water completely during hydrolysis and polycondensation, the molar ratio R (=[H_2O]/[TTB]) was adjusted to 2. The solution was aged under mild stirring for 24 h. The hydrolysis of tetrabutyl titanate results in the formation of TiO_2 nanoparticles inside the cores of the reverse micelles. The temperature of the solution during the process was kept at 30 °C. Thus, the particles prepared inside the constrained microreactors were expected to be relatively dispersed in the order of nanometers. Then the solution was charged into a 100 ml Teflon-lined stainless-steel autoclave. The autoclave was then heated to 120 °C and the temperature was kept for 24 h. After the autoclave was cooled down to room temperature, the precipitate generated at the bottom of the autoclave was separated in a centrifuge at 6000 rpm for 20 min. The residue was then washed with methanol and water several times to remove the organic contaminants and the surfactant, respectively. The product was then dried under reduced pressure at 60 °C for 5 h.

2.3. Surface treatment

Since heterogeneous catalytic reactions occur on the surfaces of catalysts, the surface conditions of catalysts are important. In order to remove organic contaminants and clean the surfaces of TiO_2 nanoparticles, two kinds of treatment (Soxhlet extractor treatment and heat treatment) were carried out after preparation of TiO_2 nanoparticles using the RM method.

Some samples were washed with methanol and deionized water using a Soxhlet extractor for 24 h, and some samples were calcined at temperature between 350 and 600 °C for 2 h under an aerated condition at a heating rate of 3 °C/min.

2.4. Photoreactivity measurement

Photocatalytic reactivity of TiO_2 nanoparticles for decomposition of toluene in the gas phase was estimated. Photocatalytic reaction was carried out using 0.1 g of TiO_2 powder. The batch reactor was filled with 125 ml of gaseous toluene at 500 ppm. A 500 W Xe lamp (Ushio Co., Ltd., SX-UI501XQ), which emits both UV light and vis light over a wide range of wavelengths, was used as a light source. Fine stainless meshes were used as neutral density filters to adjust the irradiation intensity. The amount of toluene decomposed by photocatalytic reactions was determined using a gas chromatograph (Shimadzu GC-8A, FID detector) equipped with a PEG-20M 20% Celite 545 60/80 packed glass column using a C-R8A Chromatopac instrument for data processing. In addition, the amount of CO_2 evolved by photocatalytic reactions was determined using a gas chromatograph (Shimadzu GC-9A, FID detector) with a TCP 20% Uniport R 60/80 packed column and a MT-221 Methanizer and using a Smart Chrom (KYA Technologies Co.) data processor.

2.5. Characterization

The crystal structures of the TiO_2 nanoparticles were examined by X-ray diffraction (XRD) analyses using a JEOL JDX-3500K and Cu Kα radiation of wavelength 1.54 Å in the range 10–90° (2θ). The average grain sizes were calculated from a half peak width of the XRD peak assigned to the (1 0 1) anatase phase using Scherrer's equation. The Brunauer–Emmett–Teller (BET) surface area of the particles was determined by using a Quantachrome Autosorb-1C. In order to analyze the amount of impurity such as surfactant in the prepared TiO_2 nanoparticles, thermogravimetric analyses of the samples were carried out on a TGA instrument (Otsuka Electronics Co., Ltd., RM-102) under an aerated condition at a heating rate of 20 °C/min. The chemical structures of the organic compounds remaining on the surfaces of the prepared TiO_2 nanoparticles were analyzed by using Fourier Transformed-Infrared spectroscopy (FT-IR, Nicolet Co., Magna760). The size and shape of the TiO_2 nanoparticles were observed by using an H-9000NAR transmission electron microscope (TEM). Diffuse reflectance spectra of the TiO_2 nanoparticles were recorded using a UV–vis DH-2000-BAL (UV–vis spectrometer, Mikropack Co.).

3. Results and discussion

3.1. Variation with water content, W_o

XRD patterns and TEM micrographs of TiO_2 nanoparticles prepared by the RM method at various water contents are shown in Figs. 1 and 2, respectively. As shown in Fig. 1, the crystal structures of TiO_2 nanoparticles were the anatase phase except for the TiO_2 particles prepared without hydrothermal treatment,

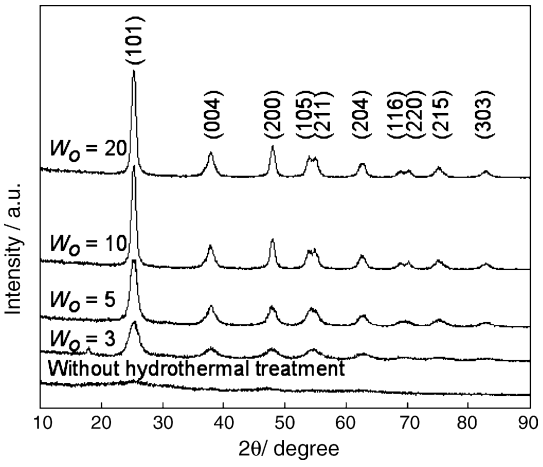

Fig. 1. XRD patterns of TiO_2 nanoparticles obtained from reverse micelle solutions with various water contents.

which were amorphous. The XRD data also showed that the crystallinity of TiO_2 nanoparticles increased with an increase in the water content. The average crystalline sizes of TiO_2 nanoparticles having the anatase phase can be calculated by applying Scherrer's equation to the anatase (1 0 1) diffraction peak as shown in Table 1. The particle size was changed by changing the water content of RM media, W_o. These tendencies of particles size were also supported by TEM analyses as shown in Fig. 2. The dispersibility of particle size of the prepared TiO_2 was narrow with each water content in RM media. Spherical or spheroid-shaped TiO_2 nanoparticles wereobserved by TEM. Additionally, HRTEM images of the TiO_2 nanoparticles prepared by the RM method at various water contents are shown in the left column of Fig. 2. The clear lattice images of TiO_2 nanoparticles having the anatase phase were observed. These results suggest that the crystallinity of TiO_2 nanoparticles prepared by the RM method was improved after hydrothermal treatment. The particle size increased with increasing water content and reached a plateau when W_o was larger than 10. When water content was higher than this value ($W_o = 10$), the average particle size did not drastically change. These features were also observed in the case of metal particles, such as copper, prepared under similar conditions [35]. In addition, the surface area of TiO_2 nanoparticles obtained by the RM method increased with decreasing W_o. The surface area reached about 300 m^2/g when W_o was lower than 3.

The particle size was strongly affected by the water content and structure inside water pools in RM media. When the volume of W_o was small, the number of water molecules per surfactant molecules was too small to hydrate head polar groups. These

Table 1
Physical properties of TiO_2 nanoparticles prepared by RM method

W_o	Structure	Crystalline size (nm)	Surface area (m^2/g)
3	Anatase	5.3	298
5	Anatase	6.9	245
10	Anatase	9.6	201
20	Anatase	10.6	187

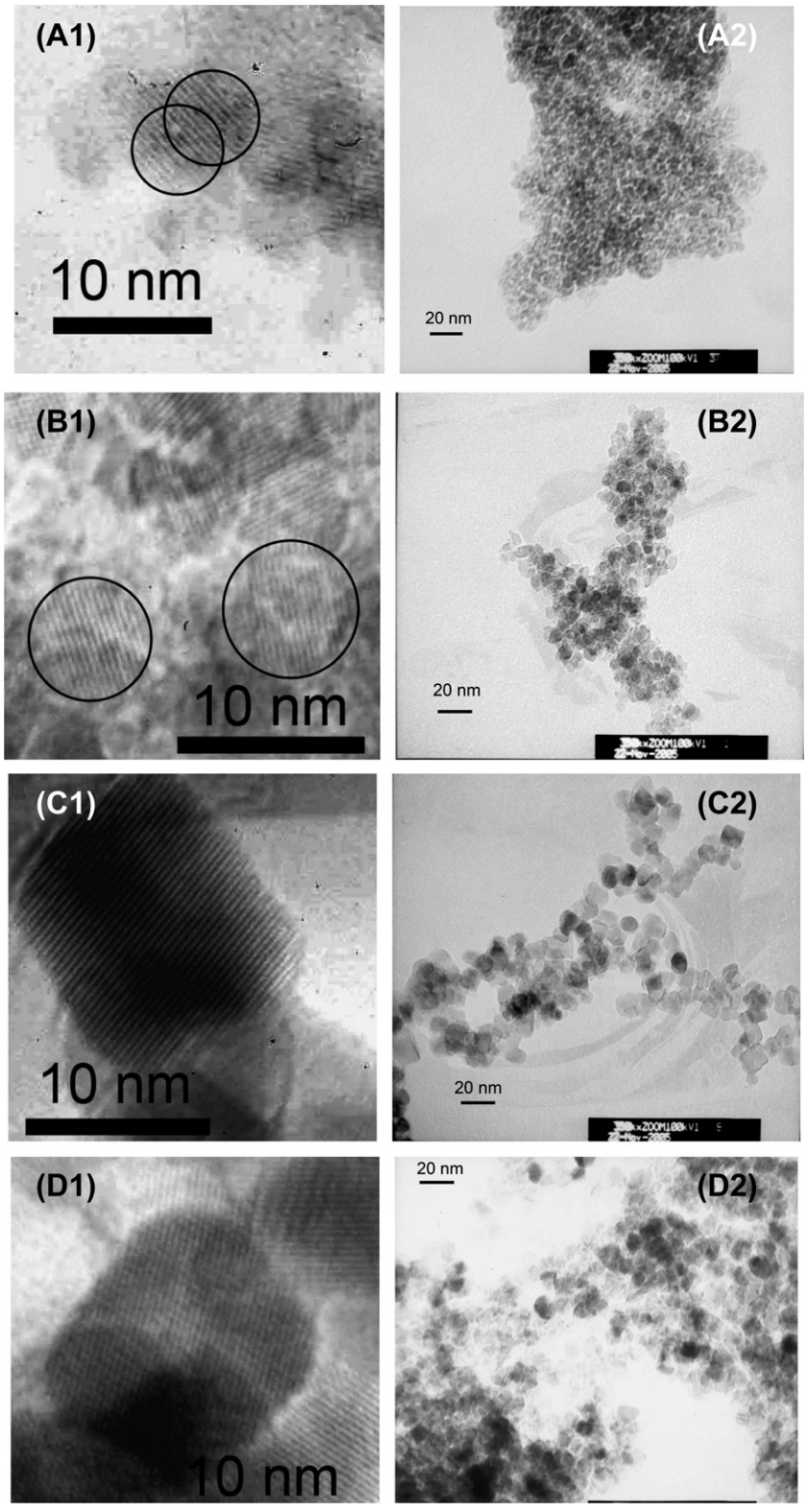

Fig. 2. HRTEM (A1–D1) and TEM (A2–D2) images of products obtained from reverse micelle solutions with various water contents: (A) $W_o = 3$, (B) $W_o = 5$, (C) $W_o = 10$ and (D) $W_o = 20$.

conditions induced strong interactions between water molecules and the head polar groups of the surfactants. The water molecules can be presumably considered as "bound" [36]. When the water content was increased, the condition of water in the water pool would be changed from "bound" to "free" [36]. In our system, the condition of water in water pools in RM media may have been changed to bulk water phase when water content (W_o) reached about 10–20.

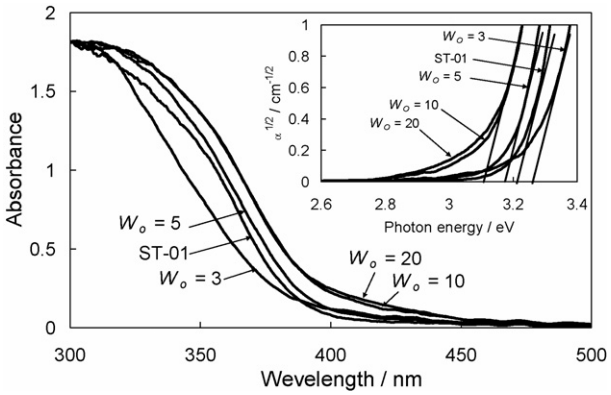

Fig. 3. UV–vis spectra and plots of the square root of the Kubelka–Munk function against the photon energy of TiO_2 particles obtained by the RM method with various water contents, W_o.

The diffuse reflectance spectra of TiO_2 nanoparticles prepared by the RM method at various water contents are shown in Fig. 3. The absorption band edge is strongly related with TiO_2 particle size less than 10 nm in diameter [37,38]. TiO_2 is an indirect gap semiconductor [39], and the band gaps of TiO_2 prepared by the RM method can also be estimated from the tangent lines in the plots of the square root of the Kubelka–Munk functions against the photon energy [40], as shown in the insert to Fig. 3. The tangent lines extrapolated to $\alpha^{1/2} = 0$ indicated that band gaps of the samples were between 3.26 and 3.12 eV. Weak absorption at 400–500 nm was observed in the case of TiO_2 nanoparticles at $W_o = 10$ and 20 because of the surface state [41].

3.2. Surface treatment

After hydrothermal treatment, the TiO_2 nanoparticles prepared by the RM method were washed with alcohol and water several times to remove organic contaminants such as the surfactant adsorbed on the surfaces of the nanoparticles. However, organic compounds still remained on the surfaces of TiO_2 nanoparticles after the treatment. These were confirmed by the observation of FT-IR spectra as discussed later. Therefore, two kinds of treatment, Soxhlet extractor treatment and heat treatment, were carried out in order to remove organic contaminants adsorbed on TiO_2 nanoparticles.

3.2.1. Soxhlet extractor treatment

When the sample was washed without soxhlet extractor treatment or heat treatment, bands at 1160 and 1240 cm^{-1} that are assigned to asymmetric and symmetric stretching vibration of C–O–C groups originated from residual organic surfactants as shown in Fig. 4.

When TiO_2 nanoparticles were washed with soxhlet extractor treatment, broad bands at 1630 cm^{-1} [42] and 3300 cm^{-1} assigned to physicosorbed water and stretching vibration of O–H groups, respectively, were observed. No peak attributable to organic compounds was observed. Consequently, we concluded that organic contaminants adsorbed on TiO_2 nanoparticles were completely removed after the treatment.

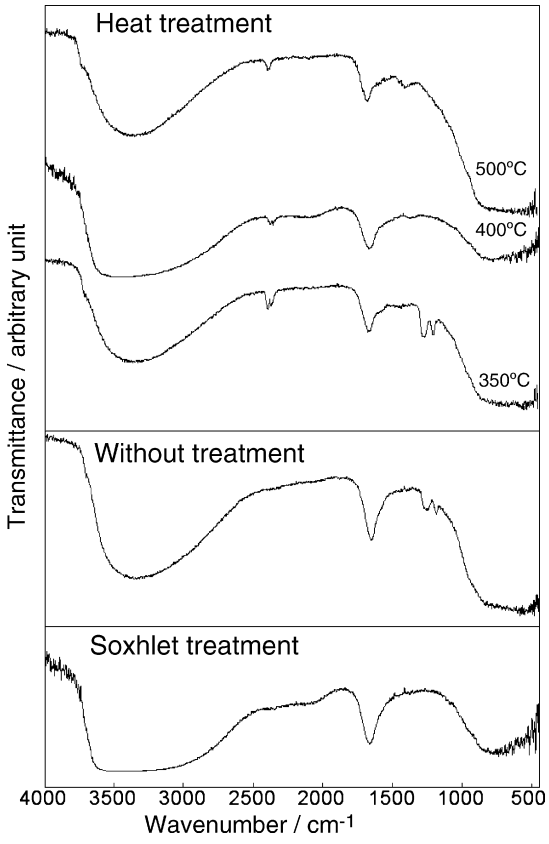

Fig. 4. FT-IR spectra of the prepared TiO_2 followed by surface treatment: $W_o = 5$, heat-treatment time 2 h, Soxhlet treatment, without treatment.

3.2.2. Heat treatment

The intensities of peaks assigned to organic contaminants in FT-IR spectra decreased with an increase in calcinations temperature. No peak that is due to residual organic compounds was observed when the sample was calcined at temperatures higher than 400 °C. As shown in Table 2, TiO_2 nanoparticles were hardly sintered up to a temperature of 400 °C. In addition, the anatase phase was stable even when TiO_2 nanoparticles were calcined at 600 °C. No phase transition from anatase to rutile took place at this temperature. This implies that the prepared TiO_2 was considerably thermostable.

These results indicate that the two kinds of the treatment (Soxhlet extractor treatment and heat treatment) are effective in removing organic contaminants that remain on the surfaces of TiO_2 nanoparticles.

Table 2
Physical properties of prepared TiO_2 particles calcined at various temperatures for 2 h

Preparation Condition	Calcination Temperature (°C)	Structure	Crystalline size (nm)	Surface area (m^2/g)
$W_o = 5$, $R = 2$	–	Anatase	6.9	245
	350	Anatase	6.5	277
	400	Anatase	7.7	186
	500	Anatase	12.0	108
	600	Anatase	42.3	45

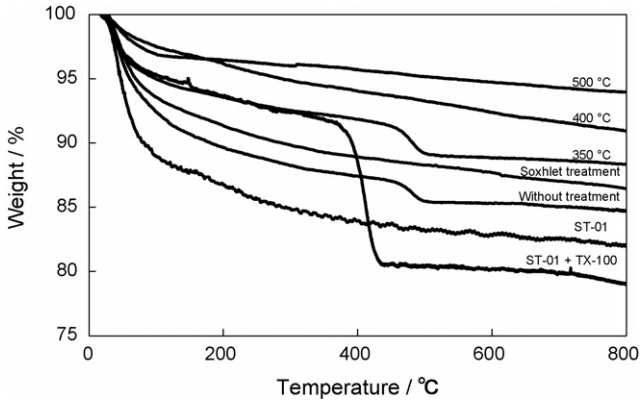

Fig. 5. TGA curves of TiO_2 particles followed by surface treatment: $W_o = 5$, heat-treatment time 2 h, Soxhlet treatment, without treatment.

3.3. TG analyses of TiO_2 nanoparticles

Fig. 5 shows TG curves of the prepared TiO_2 nanoparticles after the treatments (Soxhlet extractor treatment and heat treatment), pure TiO_2 (ST-01), and the mixture of pure TiO_2 and the surfactant (Triton X-100). The TG curves were measured in air in the temperature range from RT to 800 °C. The TG curves of the pure TiO_2 itself indicated a weight loss below 300 °C that was attributable to dehydration and desorption of water from the surfaces of TiO_2 particles. On the other hand, a mixture of pure TiO_2 and the surfactant showed an additional large weight loss at temperatures between 380 and 425 °C in TG curves. This was ascribed to combustion of the surfactant that was mixed with TiO_2 nanoparticles. The TG curve of prepared TiO_2 nanoparticles without treatment showed weight loss at temperatures between 450 and 490 °C. Weight loss in TG curves for prepared TiO_2 nanoparticles with heat treatment at 350 °C was also observed. The temperature where weight loss of the prepared TiO_2 occured was higher than that for the mixture of pure TiO_2 and the surfactant. The surfactants used for the preparation of TiO_2 nanoparticles are thought to be oxidized to form some organic contaminants whose combustion temperature may be higher than that of the original surfactant. The weight losses for prepared TiO_2 are due to the combustion of organic contaminants remaining on the surfaces of TiO_2 nanoparticles. On the other hand, TiO_2 nanoparticles with heat treatment at temperatures higher than 400 °C do not show any weight loss in TG curves. These results suggested that organic contaminants remaining on the surfaces of the prepared TiO_2 nanoparticles were completely removed after heat treatment at a temperature higher than 400 °C. The results obtained from FT-IR analyses, as mentioned in the former section, are consistent with those obtained from TG measurements.

3.4. Photocatalytic activity

As mentioned in the former section, Soxhlet extractor treatment and heat treatment were used to remove organic contaminants remaining on the surfaces of TiO_2 nanoparticles. Photocatalytic activity of each sample for decomposition of toluene in the gas phase was evaluated using TiO_2 nanoparticles prepared by the RM method after the two kinds of treatment. The photocatalytic activities and physical properties of the TiO_2 nanoparticles prepared by the RM method are listed in Tables 3 and 4.

Table 3
Physical properties of TiO_2 nanoparticles prepared at various water contents using RM method

Sample no.	W_o	Structure	Crystalline size (nm)		Surface area (m^2/g)	
			Neat[a]	Calcination[b]	Neat[a]	Calcination[b]
1	3	Anatase	5.3	5.3	298	206
2	5	Anatase	6.9	7.7	245	186
3	10	Anatase	9.6	11.6	201	151
4	20	Anatase	10.6	11.4	187	129
ST-01	–	Anatase	7.8	11.3	390	129

[a] Soxhlet treatment.
[b] Calcination temperature: 400 °C, calcination time: 2 h.

In the case of TiO_2 nanoparticles with Soxhlet extractor treatment, TiO_2 nanoparticles prepared by the RM method under the condition of $W_o = 5$ showed the highest activity for the degradation of toluene among the samples at different W_o values. The activities of TiO_2 nanoparticles prepared by the RM method increased with an increase in surface areas in the range of $W_o = 5$–20. Adsorptivity of toluene on the surfaces of TiO_2 nanoparticles was improved with an increase in surface area of TiO_2 photocatalysts. The photocatalytic activity of TiO_2 nanoparticles prepared under the condition of $W_o = 3$ was lower than that prepared under the condition of $W_o = 5$ because water pools in the RM media were too small to crystallize TiO_2 particles under the condition of $W_o = 3$.

When the heat treatments of TiO_2 nanoparticles were performed, the activity for degradation of toluene improved even though the surface area decreased. The crystallinity of TiO_2 nanoparticles was improved by heat treatment, resulting in a reduction in recombination centers such as a kink or defect of oxygen between electrons and holes. In addition, the tendency of the photocatalytic activity of TiO_2 nanoparticles prepared by the RM method with different water contents did not change even after the heat treatment. These results suggest that the balance between particle size, surface area, and crystallinity is impor-

Table 4
Photocatalytic activities of TiO_2 nanoparticles prepared at various water contents using RM method

Sample no.	Degradation of toluene $k \times 10^4$ (s^{-1})[a]		CO_2 evolution (ppm/s)	
	Neat[b]	Calcination[c]	Neat[b]	Calcination[c]
1	0.40	0.79	0.023	0.052
2	1.04	1.43	0.029	0.053
3	0.93	1.06	0.029	0.054
4	0.80	0.82	0.037	0.061
ST-01	1.23	1.30	0.044	0.044

[a] Apparent first-order constant (k) of photocatalytic degradation of toluene.
[b] Soxhlet treatment.
[c] Calcination temperature: 400 °C, calcination time: 2 h.

tant for TiO_2 nanoparticles to exhibit photocatalytic activity for decomposition of toluene.

On the other hand, for the evolution of CO_2, the sample with $W_o = 20$ showed the highest activity among the TiO_2 nanoparticles. During decomposition of toluene, oxidized compounds such as benzoic acid or dicarboxylic compounds obtained from ring-opening reaction of toluene, which are more stable than toluene, were thought to have accumulated on the surfaces of TiO_2 nanoparticles. This retards decomposition of toluene because stable reaction intermediates occupy the active sites on the surfaces of TIO_2 nanoparticles. The discrepancy between degradation of toluene and CO_2 evolution is due to the generation of stable reaction intermediates that are hardly oxidized compounds compared to toluene [43]. Larger TiO_2 particles show higher oxidation activity because band bending is necessary to enhance the oxidation power [44,45]. Therefore, decomposition of the reaction intermediates to form CO_2 in the gas phase, proceeds efficiently on large TiO_2 particles ($W_o = 20$).

The photocatalytic activity of TiO_2 nanoparticles prepared by the RM method under the condition of $W_o = 5$ with heat treatment for decomposition of toluene and evolution of CO_2 is higher than that of commercially available anatase fine particles (ST-01), one of the most active photocatalysts for degradation of organic compounds in the gas phase.

4. Conclusions

Nanosized pure TiO_2 particles with high crystallinity, large surface area and high thermostability were prepared by hydrolysis of tetrabutyl titanate in water/TX-100/isooctane reverse micelle solutions as reaction media followed by hydrothermal treatment for improvement of crystallinity. The size of TiO_2 nanoparticles can be controlled by changing the water content of the reverse micelle solution. The key factors in determining the photocatalytic activity of TiO_2 nanoparticles for decomposition of toluene are concluded to be particle size, surface area, and crystallinity. Photocatalytic activity of TiO_2 powders for the CO_2 evolution increases with an increase in the particle size since a high oxidation power based on a large band bending in TiO_2 is required for the degradation of stable reaction intermediate such as benzoic acid, which is more stable than toluene. On the other hand, the photocatalytic activity of TiO_2 powders for degradation of toluene decreased with an increase in particle size because a high oxidation power is not necessary to the decomposition of toluene, which is easily decomposed compared to reaction intermediates such as benzoic acid. Consequently, a large surface area is the most important factor for TiO_2 nanoparticles in exhibiting a high photocatalytic activity for degradation of toluene because an excess amount of toluene is concentrated on the surfaces of fine TiO_2 particles. The results suggest that the optimum conditions (particle size) forTiO_2 nanoparticles are different for different reactants.

Acknowledgements

This work was supported by a Grant-in-Aid for Scientific Research on Priority Areas (417) from the Ministry of Education, Culture, Science, and Technology (MEXT), Japan and Nissan Science Foundation.

References

[1] A. Fujishima, K. Honda, Nature 238 (1972) 37.
[2] K. Kurihara, J.H. Fendler, J. Mol. Catal. 34 (1986) 325.
[3] D.H. Chen, J.J. Yeh, T.C. Huang, J. Colloid Interface Sci. 215 (1999) 159.
[4] S.S. Hong, M.S. Lee, G.D. Lee, React. Kinet. Catal. Lett. 80 (2003) 145.
[5] S. Shiojiri, T. Hirai, I. Komasawa, J. Chem. Eng. Jpn. 30 (1997) 137.
[6] V. Chhabra, V. Pillai, B.K. Mishra, A. Morrone, D.O. Shah, Langmuir 11 (1995) 3307.
[7] S. Shiojiri, T. Hirai, I. Komasawa, J. Chem. Eng. Jpn. 30 (1997) 86.
[8] H. Goto, Y. Hanada, T. Ohno, M. Matshmura, J. Catal. 225 (2004) 223.
[9] K. Fujiwara, T. Ohno, M. Matsumura, J. Chem. Soc., Faraday Trans. 94 (1998) 3705.
[10] T. Ohno, K. Fujihara, K. Sarukawa, F. Tanigawa, M. Matsumura, Z. Phys. Chem. 213 (1999) 165.
[11] Z.G. Zou, H. Arakawa, J. Photochem. Photobiol. A: Chem. 158 (2003) 145.
[12] R. Abe, K. Sayama, H. Arakawa, Chem. Phys. Lett. 371 (2003) 360.
[13] J. Ye, Z. Zou, H. Arakawa, M. Oshikiri, M. Shimoda, A. Matsushita, T. Shishido, J. Photochem. Photobiol. A: Chem. 148 (2002) 79.
[14] B. O'Regan, M. Grätzel, Nature 353 (1991) 737.
[15] S. Kambe, S. Nakade, T. Kitamura, Y. Wada, S. Yanagida, J. Phys. Chem. B 106 (2002) 2967.
[16] M. Lal, V. Chhabra, P. Ayyub, A. Maitra, J. Mater. Res. 13 (1988) 1249.
[17] C.S. Kim, K. Nakaso, B. Xia, K. Okuyama, M. Shimada, Aerosol Sci. Technol. 39 (2005) 104.
[18] K.D. Kim, H.T. Kim, Powder Technol. 119 (2001) 164.
[19] H. Kumazawa, H. Otsuki, E. Sada, J. Mater. Sci. Lett. 12 (1993) 839.
[20] L.K. Campbell, B.K. Na, E.I. Ko, Chem. Mater. 4 (1992) 1329.
[21] U. Selvaraj, A.V. Prasadarao, S. Komarneni, R. Roy, J. Am. Ceram. Soc. 75 (1992) 1167.
[22] T. Sugimoto, K. Okada, H. Itoh, J. Colloid Interface Sci. 193 (1997) 140.
[23] T. Masui, K. Fujiwara, K. Machida, G. Adachi, Chem. Mater. 9 (1997) 2197.
[24] E. Stathatos, P. Lianos, F. DelMonte, D. Levy, D. Tsiourvas, Langmuir 13 (1997) 4295.
[25] M. Andersson, L. Osterlund, S. Ljungstrom, A. Palmqvist, J. Phys. Chem. B 106 (2002) 10674.
[26] M. Wu, J. Long, A. Huang, Y. Luo, Langmuir 15 (1999) 8822.
[27] G. Pecchi, P. Reyes, P. Sanhueza, J. Villasenor, Chemosphere 43 (2001) 141.
[28] K. Koichi, K. Okuyama, M. Shimada, S.E. Pratsinis, Chem. Eng. Sci. 58 (2003) 3327.
[29] B. Arvan, A. Khakifirooz, R. Tarighat, S. Mohajerzadeh, A. Goodarzi, E.A. Soleimani, J. Colloid Interface Sci. 218 (1999) 23.
[30] E.R. Leboda, V.M. Gun'ko, M. Marciniak, A.A. Malygin, A.A. Malkin, W. Grzegorczyk, B.J. Trznadel, E.M. Pakhlov, E.F. Voronin, J. Colloid Interface Sci. 218 (1999) 23.
[31] D.M. Zhu, K.I. Feng, Z.A. Schelly, J. Phys. Chem. 96 (1992) 2382; Arzi, Mater. Sci. Eng. B 109 (2004) 17.
[32] T. Hirai, H. Sato, I. Komasawa, Ind. Eng. Chem. Res. 32 (1993) 3014.
[33] D.H. Chen, C.C. Wang, T.C. Huang, J. Colloid Interface Sci. 210 (1999) 123.
[34] S. Yanagida, T. Enokida, A. Shindo, T. Ahiragami, T. Ogata, T. Fukumi, T. Sakaguchi, H. Mori, T. Sakata, Chem. Lett. 10 (1990) 1773.
[35] M.P. Pileni, Langmuir 13 (1997) 3266.
[36] M.P. Pileni, J. Phys. Chem. 97 (1993) 6961.
[37] Y. Li, T.J. White, S.H. Lim, J. Solid State Chem. 177 (2004) 1372.
[38] M. Anpo, T. Shima, S. Kodama, Y. Kobokawa, J. Phys. Chem. 91 (1987) 4305.
[39] F.P. Koffyberg, K. Dwight, A. Wold, Solid State Commun. 30 (1979) 433.

[40] Y.I. Kim, S.J. Atherton, E.S. Brigham, T.E. Mallouk, J. Phys. Chem. 97 (1993) 11802.
[41] Y.C. Zhu, C.X. Ding, J. Solid State Chem. 145 (1999) 711.
[42] G. Pecchi, P. Reyes, P. Sanhueza, J. Villasenor, Chemosphere 43 (2001) 141.
[43] Y. Luo, D.F. Ollis, J. Catal. 163 (1996) 1.
[44] T. Ohno, D. Haga, K. Fujihara, K. Kaizaki, M. Matsumura, J. Phys. Chem. B 101 (1997) 6415–6419.
[45] M. Anpo, K. Chiba, M. Tomonari, S. Coluccia, M. Che, M.A. Fox, Bull. Chem. Soc. Jpn. 64 (1991) 543.